Hadroproduction of the χ_1 and χ_2 states of charmonium in 800-GeV/c proton-silicon interactions

T. Alexopoulos,[18] L. Antoniazzi,[11] M. Arenton,[17] H. C. Ballagh,[1] H. Bingham,[1] A. Blankman,[12] M. Block,[10] A. Boden,[2] G. Bonomi,[11] Z. L. Cao,[17] T. Y. Chen,[9] K. Clark,[15] D. Cline,[2] S. Conetti,[17] M. Cooper,[16] G. Corti,[17] B. Cox,[17,*] P. Creti,[7] E. C. Dukes,[17] C. Durandet,[18] V. Elia,[7] A. R. Erwin,[18] L. Fortney,[4] V. Golovatyuk,[7] E. Gorini,[7] F. Grancagnolo,[7] K. Hagan,[17] M. Haire,[13] P. Hanlet,[17] M. He,[14] G. Introzzi,[11] M. Jenkins,[15] D. Judd,[13] W. Kononenko,[12] W. Kowald,[4] K. Lau,[6] A. Ledovskoy,[17] G. Liguori,[11] J. Lys,[1] P. O. Mazur,[5] A. P. McManus,[17] S. Misawa,[1] G. H. Mo,[6] C. T. Murphy,[5] K. Nelson,[17] V. Pogosyan,[17] S. Ramachandran,[2] J. Rhoades,[2] W. Selove,[12] R. P. Smith,[5] L. Spiegel,[5] J. G. Sun,[17] S. Tokar,[3] P. Torre,[11] J. Trischuk,[8] L. Turnbull,[13] D. E. Wagoner,[13] C. R. Wang,[14] C. Wei,[14] W. Yang,[5] N. Yao,[9] N. J. Zhang,[14] and B. T. Zou[4]

(E771 Collaboration)

[1]*University of California at Berkeley, Berkeley, California 94720*
[2]*University of California at Los Angeles, Los Angeles, California 90024*
[3]*Comenius University, Bratislava, Slovakia*
[4]*Duke University, Durham, North Carolina 27706*
[5]*Fermi National Accelerator Laboratory, Batavia, Illinois 60510*
[6]*University of Houston, Houston, Texas 77204*
[7]*University and INFN of Lecce, I-73100 Lecce, Italy*
[8]*McGill University, Montreal, PQ Canada H3A 2T8*
[9]*Nanjing University, Nanjing, People's Republic of China*
[10]*Northwestern University, Evanston, Illinois 60208*
[11]*University and INFN of Pavia, I-27100 Pavia, Italy*
[12]*University of Pennsylvania, Philadelphia, Pennsylvania 19104*
[13]*Prairie View A&M, Prairie View, Texas 77446*
[14]*Shandong University, Jinan, Shandong, People's Republic of China*
[15]*University of South Alabama, Mobile, Alabama 36688*
[16]*Vanier College, St. Laurent, PQ Canada H4L 3X9*
[17]*University of Virginia, Charlottesville, Virginia 22901*
[18]*University of Wisconsin, Madison, Wisconsin 53706*

(Received 20 July 1999; published 11 July 2000)

The cross sections for the hadroproduction of the χ_1 and χ_2 states of charmonium in proton-silicon collisions at $\sqrt{s}=38.8$ GeV have been measured in Fermilab fixed target experiment 771. The χ states were observed via their radiative decay to $J/\psi\gamma$, where the photon converted to e^+e^- in the material of the spectrometer. The estimated values for the χ_1 and χ_2 cross sections for $x_F>0$ are $263\pm69(\text{stat})\pm32(\text{syst})$ and $498\pm143(\text{stat})\pm67(\text{syst})$ nb per nucleon, respectively. The resulting $\sigma(\chi_1)/\sigma(\chi_2)$ ratio of $0.53\pm0.20(\text{stat})\pm0.07(\text{syst})$, although somewhat larger than most theoretical expectations, can be accommodated by the latest theoretical estimates.

PACS number(s): 13.85.Ni, 13.85.Qk, 14.40.Gx, 25.40.Ve

Charmonium hadroproduction has provided interesting challenges to the understanding of QCD. Early attempts to describe the formation of a $c\bar{c}$ bound state, according to the *color evaporation* [1] or *color singlet* [2] models, did not provide a satisfactory description of the available data. The measurement presented here represents a significant contribution to existing $c\bar{c}$ hadroproduction data, since it is the first observation of cleanly resolved χ_1 and χ_2 states in a pN fixed target experiment.

In the color evaporation approach, the $c\bar{c}$ pair is assumed to be produced in an unbound, not necessarily colorless state. The final colorless $c\bar{c}$ state is reached via the emission of soft ''color bleaching'' gluons. Because of its semi-empirical nature, color evaporation cannot make specific predictions of the relative charmonium state production rates. Rather, it is assumed that either they are all produced at the same rate or proportionally to the number of spin states (3:5 for χ_1/χ_2 production).

The color singlet model, on the contrary, demands that the $c\bar{c}$ pair be produced in a bound colorless state and attempts to compute the rate of production for various charmonium states by taking into account the relevant quark and gluon diagrams. When dealing with χ_1 and χ_2 production by protons on a nuclear target, the contribution of antiquarks (from the nucleon sea) is small, and χ production via $q\bar{q}$ annihilation is negligible compared to gluon mediated processes. Moreover, χ_1 production by gluons is suppressed at the lowest order by the Yang [3] theorem, forbidding the production

*Corresponding author. Electronic address: cox@uvahep.phys.virginia.edu

of a spin-1 particle by two massless spin-1 quanta. So in proton induced reactions, the χ_1/χ_2 ratio is expected to be of order 5% [4].

More recently, the nonrelativistic QCD (NRQCD) factorization approach [5], which incorporates in a more rigorous fashion some of the features of the previous models, has provided a more successful description of the process. In particular, the NRQCD approach allows the initial $c\bar{c}$ state to be produced in a color octet as well as a color singlet state, but also factorizes the production process into a short distance process, where the $c\bar{c}$ pair is created, and a long distance part in which the $c\bar{c}$ pair hadronizes into the observed charmonium state. As discussed below, the most recent estimates of this model are that the χ_1 to χ_2 ratio can be as large as 30%.

The Fermilab E771 experiment utilized a large-acceptance spectrometer [6] to measure several processes containing muons in the final state. Protons of 800 GeV/c momentum were transported by the Fermilab Proton West beam line to the High Intensity Laboratory, where they hit a 24 mm thick silicon target. Operating at a beam intensity of $\approx 3.6\times 10^7$ protons per spill second, the experiment accumulated a total of 6.4×10^{11} p-Si interactions. The incoming proton beam trajectory and flux were measured by a six plane silicon detector station. The 0.26 radiation length target was composed of twelve 2 mm silicon foils separated by 4 mm. The target was followed by a microvertex detector consisting of fourteen 300 μm thick silicon planes that, while not used in the analysis presented here, contributed an additional $0.045X_0$ to the target region radiation length.

The spectrometer's tracking system consisted of seven multi-wire proportional chambers and three drift chambers upstream plus three drift chambers and six combination drift/pad/strip chambers downstream of a dipole analysis magnet which provided an 821 MeV/c p_t kick in the horizontal plane. Downstream of the wire chamber system, an electromagnetic calorimeter consisting of an active converter and 396 scintillating glass and lead glass blocks was used for electron and positron identification. The final element of the spectrometer, a set of three planes of resistive plate counters (RPC's) segmented into 512 readout pads and sandwiched between layers of steel and concrete absorbers, provided muon identification. The material in the absorber walls represented an energy loss of 10 GeV in the central region and 6 GeV in the outer region of the detector for the incident muons.

A dimuon trigger [7] selected events with a J/ψ in the final state via the decay $J/\psi\rightarrow\mu^+\mu^-$. A trigger muon was defined as the triple coincidence of the *OR* of 2×2 pads in the first RPC plane and the *OR* of 6×6 pads in the second and third RPC planes in projective arrangements. A dimuon trigger was defined as two such triple coincidences. The trigger reduced the 1.9 MHz interaction rate by a factor of $\approx 10^4$, selecting approximately 1.3×10^8 dimuon events to be written to tape.

The seed for muon track reconstruction was provided by the RPC triple coincidences. The roads formed by the pads involved in the coincidences were projected into the rear chamber set, identifying a region in which to search for candidate muon tracks. Muon tracks reconstructed in the rear chamber set were then matched with tracks found in the front chamber set by requiring a good front-rear linking χ^2. The muon pairs were required to come from a common vertex. About 50 000 dimuon events survived the reconstruction process and cuts.

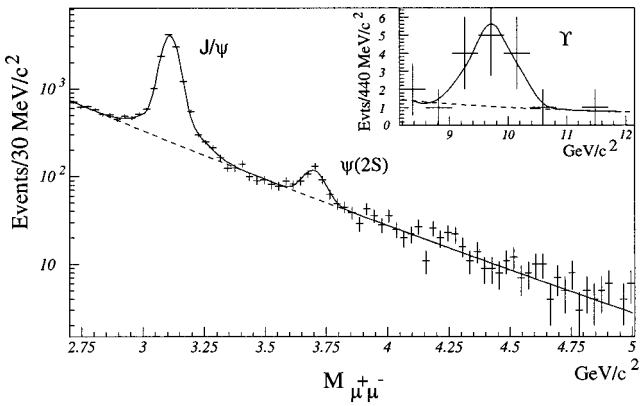

FIG. 1. Opposite sign dimuon mass spectrum. The solid line is a fit to the signal plus background and the dashed line is a fit to the background only. The inset shows the Υ signal.

Figure 1 shows the resulting dimuon mass spectrum containing peaks corresponding to the J/ψ, $\psi(2S)$, and Υ (inset). Superimposed on the dimuon mass spectrum is a fit to the data obtained with the sum of two Gaussians for the J/ψ peak, a single Gaussian for the $\psi(2S)$, and the form $(a/m^3_{\mu\mu})\exp(-bm_{\mu\mu})$ for the continuum background. The two Gaussians fit to the J/ψ peak is a good approximation (as confirmed by Monte Carlo simulations) to a nonconstant mass resolution, caused by the confusion associated with increases in hit density near the beam region. The number of J/ψ's and $\psi(2S)$'s after background subtraction was $11\,660\pm 139$ and 218 ± 24, respectively [8].

Events in a window of ± 100 MeV/c^2 around the J/ψ mass were refit varying the muon momenta within measurement errors, with the constraint that the invariant mass of the pair be equal to J/ψ mass. The resulting dimuon event sample was then inspected to search for e^+e^- pairs that might be the result of conversions of photons from $\chi\rightarrow J/\psi\gamma$ decays. Dimuon events which contained pairs of tracks matching the topology of a $\gamma\rightarrow e^+e^-$ conversion in the target region—collinear before the magnet in both bend and non-bend projections, collinear in the non-bend plane and coplanar in the bend plane after the magnet—were then designated as χ decay candidates.

All electron-positron pair candidates were required to satisfy additional conditions. At least one of the two track candidates was required to be associated with an energy deposition in the calorimeter consistent with an electro-magnetic shower. In addition, the total transverse momentum of the e^+e^- pair in the rear of the magnet was required to be zero (within the resolution of the spectrometer) relative to the common e^+e^- trajectory in front of the magnet. To quantify how well a pair fitted the $\gamma\rightarrow e^+e^-$ hypothesis, a χ^2 was formed,

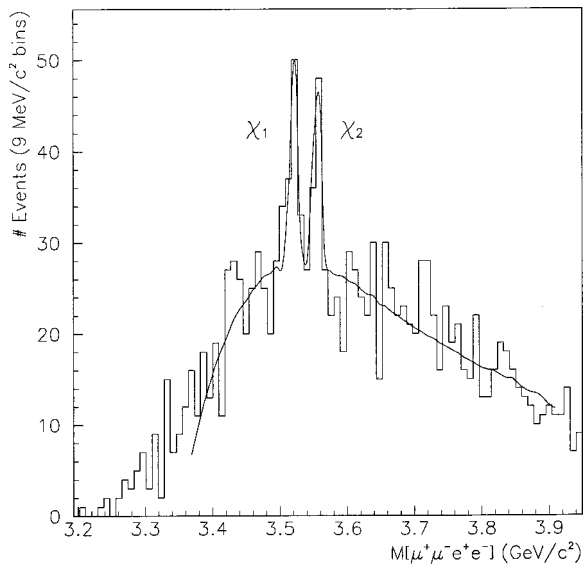

FIG. 2. $J/\psi e^+e^-$ invariant mass. The solid line shows a fit to a polynomial background plus two Gaussians of equal width.

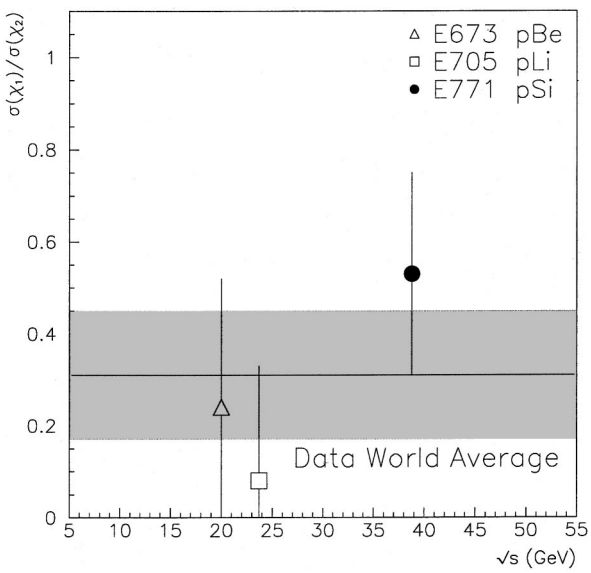

FIG. 3. $\sigma(\chi_1)/\sigma(\chi_2)$ in proton-nucleon interactions. Results from this experiment (E771) are shown, together with the two existing results and the world average with 1σ errors.

$$\chi^2=\frac{(a_{x1}-a_{x2})^2}{\sigma_{ax1}^2+\sigma_{ax2}^2}+\frac{(a_{y1}-a_{y2})^2}{\sigma_{ay1}^2+\sigma_{ay2}^2}+\frac{(b_{y1}-b_{y2})^2}{\sigma_{by1}^2+\sigma_{by2}^2} \qquad (1)$$

where a_{x1} and a_{x2} are the electron and positron track intercepts at the magnet in the bend plane, a_{y1} and a_{y2} the track intercepts in the non-bend plane, b_{y1} and b_{y2} the track slopes in the non-bend plane, and the σ's are the measurement errors on these quantities. The electron-positron candidate with the smallest χ^2 in a given event was designated as a photon conversion candidate. Additional cuts requiring a good χ^2, the transverse momentum of the parent photon to be between 250 and 700 MeV/c, and the invariant mass squared of the e^+e^- pair to be less than 3000 $(\mathrm{MeV}/c^2)^2$ were applied to maximize signal to background in the final sample of events containing both a J/ψ and a photon conversion.

The J/ψ e^+e^- invariant mass shown in Fig. 2 was calculated using the electron and positron momenta obtained from the tracking system. Clear χ_1 and χ_2 signals can be seen. The background to the χ_1 and χ_2 was well described by uncorrelated e^+e^- and J/ψ combinations: the solid line of Fig. 2 was obtained by fitting two Gaussians plus a polynomial background. The polynomial background was obtained by fitting the mass distributions of J/ψ's and e^+e^-'s extracted from different events. The numbers of χ_1 and χ_2 obtained from the fit are 33 ± 9 and 33 ± 10, respectively. The fitted width is 5.2 ± 2.0 MeV/c^2 for both the χ_1 and χ_2 peaks.

To determine the total cross section for χ_1 and χ_2 production, the overall acceptance times efficiency for photon conversion and for electron-positron acceptance and reconstruction efficiency had to be determined. To accomplish this, a Monte Carlo sample of $\chi\to J/\psi\ \gamma$, $J/\psi\to\mu^+\mu^-$ decays was generated using PYTHIA [9]. The photon and the muons were then propagated through a GEANT [10] simulation of the E771 detector, including γ conversion, scattering, bremsstrahlung and dE/dx. Hits from the Monte Carlo tracks obtained by this prescription were then inserted into actual dimuon trigger events to simulate realistically backgrounds and losses in pattern recognition due to confusion from noise hits and other tracks. Measured detector efficiencies were also applied to the inserted hits. These hybrid Monte Carlo and data events were analyzed in a manner identical to the data in order to determine acceptances and tracking efficiencies.

Rather than simulating the response of the electromagnetic calorimeter to $e^\pm$ in detail in a Monte Carlo simulations, the efficiency of matching an electron or positron candidate to a shower in the calorimeter was determined using a large sample of electron-positron pairs from photon conversions in minimum bias events. A sample of e^+e^- pairs with kinematics similar to those of the χ e^+e^- pairs was collected using very tight cuts to ensure an e^+e^- identity. This sample was then subjected to the same constraints as those applied in the χ analysis. The acceptance for $\gamma\to e^+e^-$ was 12.2% and the efficiency for reconstruction and physics analysis of the e^+e^- 18.6%. The conversion probability for χ photons was 36.3%, resulting in an overall acceptance times efficiency times conversion probability for photons from χ decay of $(8.24\pm0.4)\times10^{-3}$. The region of x_F acceptance of the spectrometer for χ's was between $x_F=0$, and $x_F=0.25$.

Using the $\gamma\to e^+e^-$ acceptance and efficiency, the measured branching ratios for χ_1 and χ_2 into $J/\psi\ \gamma$ [11], the measured $J/\psi\ pN$ forward cross section [8] at $\sqrt{s}=38.8$ GeV and the number of observed χ_1, χ_2 and $J/\psi\to\mu^+\mu^-$, the absolute χ_1 and χ_2 cross sections for $x_F>0$ were calculated to be $\sigma(\chi_1)=263\pm69(\mathrm{stat})\pm32(\mathrm{syst})$ nb/nucleon and $\sigma(\chi_2)=498\pm143(\mathrm{stat})\pm67(\mathrm{syst})$ nb/nucleon, respectively. The main contributions to the systematic errors came from the error on the J/ψ cross section (9%), the uncertainty in the knowledge of the cut efficiencies (5%) and the errors on the branching ratios for χ_1 (6%) and χ_2 (8%).

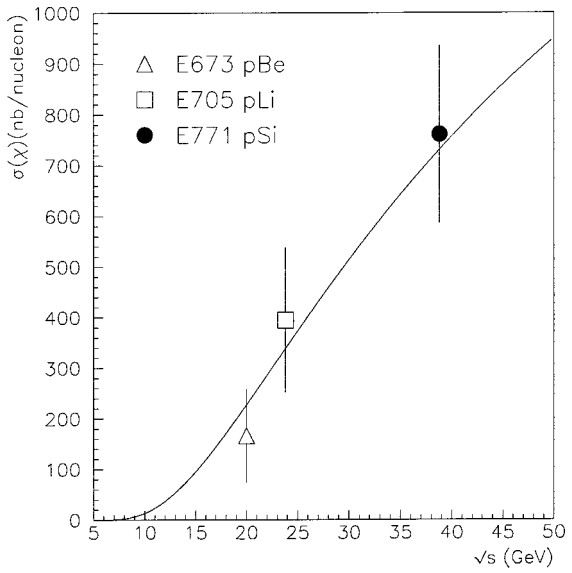

FIG. 4. $\sigma(\chi)$ vs $\sqrt{s}$ in pN interactions. Superimposed is a fit to a threshold production parametrization described in the text; $\sigma(\chi)$ is the sum of the χ_1 and χ_2 cross sections where the E673 data point has been obtained from the published χ_1 cross section and ratio of χ_2/χ_1.

The contribution to the systematic error due to the model dependence of heavy quark production was also investigated. The χ cross sections quoted above are based on our J/ψ cross section measurement [8]. The systematic error in the J/ψ cross section included model dependence and is incorporated in the quoted χ systematic errors. In addition, effects specific to χ production have been investigated. The color singlet model for chi production [12], as incorporated in PYTHIA in our Monte Carlo simulation, was modified by varying the wave function at the origin and the derivative of the wave function by $\pm 30\%$. The corresponding $\pm 2\%$ change in the χ acceptance and χ cross sections is included in the systematic error.

Using the production cross sections for χ_1 and χ_2, the ratio of the χ_1 to χ_2 production cross sections was determined to be $\sigma(\chi_1)/\sigma(\chi_2) = 0.53 \pm 0.20(\text{stat}) \pm 0.07(\text{syst})$. Combining this result with the two previous measurements of χ production by a proton beam [13], we have computed the world average (shown in Fig. 3) to be $\sigma(\chi_1)/\sigma(\chi_2) = 0.31 \pm 0.14$. This figure is consistent with the latest NRQCD estimates of ≈ 0.3 [14], where χ_1 production was boosted by the inclusion of higher order terms in the velocity expansion [15].

Finally, the energy dependence of the combined χ_1 and χ_2 production near threshold was compared to the corresponding quantity for J/ψ production. In Ref. [16] J/ψ production data from 17 pN experiments were fit as a function of $\sqrt{s}$ between 8 and 52 GeV. The J/ψ production data near threshold was well represented by the function $\sigma(\sqrt{s})_{J/\psi} = \sigma_0(1 - M_{J/\psi}/\sqrt{s})^{\beta}$, with $\sigma_0 = 1.0 \pm 0.1$ μb/nucleon and $\beta = 11.8 \pm 0.5$. To check whether χ production has similar dynamics as J/ψ production, the sum of the χ cross sections has been fit to a similar parametrization with β fixed to the J/ψ value and M_{χ} replacing $M_{J/\psi}$. The fit, shown in Fig. 4, illustrates the similarity of the J/ψ and χ production at threshold. The fit yields $\sigma_0 = 2.3 \pm 0.4$ μb/nucleon for the asymptotic $\sigma(\chi)$ cross section.

We wish to thank Fermilab, the U.S. Department of Energy, the National Science Foundation, the Istituto Nazionale di Fisica Nucleare of Italy, the Natural Science and Engineering Research Council of Canada, the Institute for Particle and Nuclear Physics of the Commonwealth of Virginia, and the Texas Advanced Research Program for their support.

[1] M. B. Einhorn and S. D. Ellis, Phys. Rev. D **12**, 2007 (1975); H. Fritzsch, Phys. Lett. **67B**, 217 (1977); M. Glück, J. F. Owens, and E. Reya, Phys. Rev. D **17**, 2324 (1978).

[2] C. H. Chang, Nucl. Phys. **B172**, 425 (1980); E. L. Berger and D. Jones, Phys. Rev. D **23**, 1521 (1981); R. Baier and R. Rückl, Phys. Lett. **102B**, 364 (1981); Z. Phys. C **19**, 251 (1983).

[3] C. N. Yang, Phys. Rev. **77**, 242 (1950).

[4] M. Beneke and I. Z. Rothstein, Phys. Rev. D **54**, 2005 (1996); G. A. Schuler, Z. Phys. C **71**, 317 (1996).

[5] G. T. Bodwin, E. Braaten, and G. P. Lepage, Phys. Rev. D **51**, 1125 (1995). For a recent review and a more complete list of references see also [14].

[6] T. Alexopoulos *et al.*, Nucl. Instrum. Methods Phys. Res. A **376**, 375 (1998).

[7] L. Antoniazzi *et al.*, Nucl. Instrum. Methods Phys. Res. A **360**, 334 (1995).

[8] T. Alexopoulos *et al.*, Phys. Lett. B **374**, 271 (1996).

[9] T. Sjöstrand, Report No. CERN-TH.7112/93.

[10] CERN Applications Software Group, CERN Program Library Long Writeup W5013.

[11] Particle Data Group, C. Caso *et al.*, Eur. Phys. J. C **3**, 1 (1998).

[12] E. W. N. Glover, A. D. Martin, and W. J. Stirling, Z. Phys. C **38**, 473 (1988).

[13] D. A. Bauer *et al.*, Phys. Rev. Lett. **54**, 753 (1985); L. Antoniazzi *et al.*, Phys. Rev. D **49**, 543 (1994).

[14] M. Beneke, *The Strong Interaction, From Hadrons to Protons*, edited by J. Chan, L. DePorcel, and L. Dixon (Stanford University Press, Stanford, CA, 1996), p. 549; hep-ph/9703429.

[15] S. Gupta and P. Mathews, Phys. Rev. D **55**, 7144 (1997); **56**, 3019 (1997).

[16] T. Alexopoulos *et al.*, Phys. Rev. D **55**, 3927 (1997).